

# ***MMTV-cre*-mediated *fur* inactivation concomitant with *PLAG1* proto-oncogene activation delays salivary gland tumorigenesis in mice**

LIESELOT DE VOS<sup>1</sup>, JEROEN DECLERCQ<sup>1</sup>, GEORGINA GALICIA ROSAS<sup>2</sup>,  
BOUDEWIJN VAN DAMME<sup>3</sup>, ANTON ROEBROEK<sup>4</sup>, FONS VERMORKEN<sup>1</sup>,  
JAN CEUPPENS<sup>2</sup>, WIM VAN DE VEN<sup>1</sup> and JOHN CREEMERS<sup>1</sup>

<sup>1</sup>Laboratory for Molecular Oncology, Department of Human Genetics, <sup>2</sup>Division of Clinical Immunology,  
<sup>3</sup>Department of Morphology and Molecular Pathology, <sup>4</sup>Laboratory for Developmental and Molecular Genetics,  
Department of Human Genetics, Katholieke Universiteit Leuven, B-3000 Leuven, Belgium

Received December 6, 2007; Accepted January 25, 2008

**Abstract.** Proprotein convertases are serine endoproteases implicated in the proteolytic processing of a large variety of regulatory proteins. An important role of proprotein convertases in tumorigenic processes has been suggested by various studies. In this study, the role of the proprotein convertase furin in *PLAG1* proto-oncogene-induced salivary gland tumorigenesis was investigated. *PLAG1* overexpression in salivary glands has previously been shown to result in salivary gland tumors in 100% of mice within 5 weeks after birth. *MMTV-cre*-mediated inactivation of *fur* without overexpression of *PLAG1* caused smaller but histologically normal salivary glands. Moreover, the lymph nodes close to the salivary glands were enlarged, and histology showed that they had activated follicles. When genetic ablation of 1 or 2 alleles of *fur* and overexpression of the *PLAG1* transgene were simultaneously achieved, a significant delay in tumorigenesis was observed. Collectively, these results suggest an important role for furin in *PLAG1*-induced salivary gland tumorigenesis in mice.

## **Introduction**

Proprotein convertases (PCs) are serine endoproteases implicated in the activation of a large variety of regulatory proteins by cleavage at basic motifs. An important role of PCs in tumorigenesis has been suggested by the fact that PCs are implicated in the proteolytic maturation and activation of growth factors and their receptors, adhesion molecules, metalloproteinases, and angiogenic factors (1-5). Furin (the prototype PC) and the other PCs are frequently upregulated in tumor tissue (3). Also, furin expression increases as the tumor behaves more aggressively (6). Therefore, PC expression might be a valuable prognostic factor. Recently, a greater understanding of the signaling pathway that regulates furin expression has uncovered a complex interplay between tumorigenesis enhancers transforming growth factor  $\beta$  (TGF- $\beta$ ) (through Smad and ERK), hypoxia-inducible factor 1 and furin (3). A number of *in vitro* studies have indicated that cell growth, cell survival and cell invasion decreased when furin, and to some extent other PCs, were inhibited and increased when furin was overexpressed (7-13). In rodents, it was shown that there was a delayed and lower incidence of tumorigenesis and reduced tumor size when PC inhibitors were transfected into rat Leydig tumor cells, (HN)SCC, HT-29 and astrocytoma cells (7-12), while there was an increased tumor size when furin was overexpressed (13). Besides that, reduced tumor vascularization was reported when PCs were inhibited (9). This suggests that PCs can function as a potential target for tumor therapy.

The general *fur* knockout mouse displays early embryonic lethality (the knockouts die between E10.5 and E11.5), due to failure of ventral closure and axial rotation (14). This is probably caused by an impaired processing of signaling proteins responsible for ventral closure and embryonic turning, such as members of the TGF- $\beta$  family. Therefore, a conditional *fur* knockout mouse was made in our laboratory, where the essential exon 2 of *fur* is flanked by *loxP* sites by homologous recombination (15). When these mice were crossed with *MX-*

---

*Correspondence to:* Dr Wim Van de Ven, Laboratory for Molecular Oncology, Department of Human Genetics, K.U. Leuven, Herestraat 49/602, B-3000 Leuven, Belgium  
E-mail: wim.vandeven@med.kuleuven.be

*Abbreviations:* PC, proprotein convertase; TGF- $\beta$ , transforming growth factor  $\beta$ ; *PLAG1*, pleomorphic adenoma gene 1; MMTV, mouse mammary tumor virus; QRT-PCR, quantitative real-time PCR; GAPDH, glyceraldehyde 3-phosphate dehydrogenase; H&E, haematoxylin and eosin; SMA, smooth muscle actin; CK8/18, cytokeratin 8/18; FACS, fluorescence-activated cell sorting; Th, T-helper; Tc, T-cytotoxic; IFN- $\gamma$ , interferon- $\gamma$ ; IGF-2, insulin-like growth factor-2; IGF-1R, insulin-like growth factor-1 receptor

*Key words:* *MMTV-cre*, *fur* inactivation, immune system, *PLAG1* proto-oncogene activation, salivary gland tumorigenesis

*cre* transgenic mice, a nearly complete ablation of *fur* in the liver of adult mice was found after a 10-day induction period with interferon (15). In sharp contrast with the general *fur* knockouts, no obvious adverse effects were found in these mice. Analysis of candidate furin substrates in liver revealed a limited redundancy of furin: the insulin receptor was still completely processed and albumin,  $\alpha$ 5-integrin, lipoprotein receptor-related protein, vitronectin and  $\alpha$ 1-microglobulin/bikunin were still processed to a variable degree.

The *pleomorphic adenoma gene 1* (*PLAG1* or *P1* in brief) is the founding member of a subfamily of zinc finger transcription factors. *PLAG1*, located on human chromosome 8q12, is a proto-oncogene and encodes a developmentally regulated protein (16). It is well established that *PLAG1* overexpression is implicated in various human neoplasias, such as pleomorphic adenomas of the salivary glands (17-19), lipoblastomas (20-22), hepatoblastomas (23), uterine leiomyomas (17), leiomyosarcomas (17) and acute myeloid leukaemia (24).

When *PLAG1* overexpression was targeted to the salivary glands of *PLAG1* transgenic mice using the *MMTV-cre* system, pleomorphic adenoma occurred (25,26) and mammary gland tumors resulted when *PLAG1* was targeted to the mammary glands (25). When *PLAG1* overexpression was controlled by *cre* using the *aP2*-promoter, cavernous angiomas arose in *PLAG1* transgenic mice (27).

To study the impact of targeted *PLAG1* overexpression in the salivary glands, two independent *PLAG1* transgenic mouse strains, PTMS1 and PTMS2, in which the activation of *PLAG1* overexpression can be mediated by the *cre* enzyme, were crossed with B6129-Tgn(*MMTV-LTR/cre*)1Mam transgenic mice (*mouse mammary tumor virus-cre* or *MMTV-cre* or *Mcre* in brief) (28), resulting in *P1-Mcre* and *P2-Mcre* double transgenic offspring, respectively (25). One hundred percent of *P1-Mcre* mice developed salivary gland tumors ~5-6 weeks after birth. These tumors bore various hallmarks of human pleomorphic adenoma of the salivary glands. The histological features included epithelial structures in a myxoid stroma in which also myoepithelial cells were observed, squamous differentiation with keratin pearls, sebaceous differentiation and mitotic figures. In older *P1-Mcre* mice, features such as necrosis, haemorrhages and cellular polymorphism indicated malignancy, and lung metastases were also observed. In contrast, only 6% of *P2-Mcre* mice developed such tumors and only after several months. The lower tumor incidence in *P2-Mcre* mice as compared to *P1-Mcre* mice is most likely due to different genomic integration sites of the transgene.

In this study, we investigated whether furin plays a role in *PLAG1*-induced salivary gland tumorigenesis. We used a mouse compound double conditional transgenic knockout model, where *MMTV-cre*-mediated overexpression of *PLAG1* was achieved, simultaneously with *MMTV-cre*-mediated complete or heterozygous inactivation of *fur*. Due to the low salivary gland tumor incidence in *P2-Mcre* mice, the furin impact study was only performed with *P1-Mcre* mice.

## Materials and methods

*Targeted inactivation of the fur gene in MMTV-cre transgenic conditional fur knockout mice.* The generation of a conditional

*fur* knockout mouse line has been reported previously (15). Briefly, homologous recombination was used to flank the essential exon 2 of *fur* with *loxP* sites. In this way, ES cells were derived with a *fur<sup>fllox</sup>* allele. These ES cell lines gave rise to *fur<sup>w<sup>t</sup>/fllox</sup>* mice and subsequently, the floxed *fur* allele (*fur<sup>fllox</sup>*) was turned into a *fur* null allele (*fur<sup>Δfllox</sup>*) by crossing with a general deleter *PGK-cre* transgenic mouse strain. In this way, *fur<sup>w<sup>t</sup>/Δfllox</sup>* mice were generated.

In this study, *fur<sup>w<sup>t</sup>/Δfllox</sup>* mice were crossed with B6129-Tgn(*MMTV-LTR/cre*)1Mam transgenic mice (*MMTV-cre* or *Mcre*) (Jackson's Laboratories) (28) to generate *Mcre<sup>+</sup>-fur<sup>w<sup>t</sup>/Δfllox</sup>* mice. These mice were further crossed with *fur<sup>fllox/fllox</sup>* mice to obtain *Mcre<sup>+</sup>-fur<sup>fllox/Δfllox</sup>* mice (*fur* knockout in salivary glands and other MMTV-promoter-targeted cell lineages, as discussed below), which have at least one inactivated allele of *fur* in all of their cells, and in the cell lineages where *cre* is or has been expressed, both alleles of *fur* are inactivated. Besides offspring with this genotype, offspring with the following genotypes were also generated: *Mcre<sup>+</sup>-fur<sup>w<sup>t</sup>/fllox</sup>* (*fur* heterozygote in salivary glands and other MMTV-promoter-targeted cell lineages), *Mcre<sup>+</sup>-fur<sup>fllox/fllox</sup>* (*fur* heterozygote in all cells) and *Mcre<sup>+</sup>-fur<sup>w<sup>t</sup>/fllox</sup>* (*fur* wild-type in all cells).

*MMTV-cre mediated fur inactivation concomitant with PLAG1 proto-oncogene overexpression in genetically modified mice.* The generation of a *PLAG1* transgenic founder line; PTMS1, has been reported previously (25). In order to generate compound *PLAG1* and *MMTV-cre* transgenic/*fur* knockout mice, we crossed *fur<sup>fllox/fllox</sup>* mice with PTMS1 to generate *P1<sup>+</sup>-fur<sup>w<sup>t</sup>/fllox</sup>* mice, and in parallel *MMTV-cre* transgenic mice were crossed with *fur<sup>fllox/Δfllox</sup>* mice to generate *Mcre<sup>+</sup>-fur<sup>w<sup>t</sup>/Δfllox</sup>* mice. Mating of these compound heterozygous *P1<sup>+</sup>-fur<sup>w<sup>t</sup>/fllox</sup>* and *Mcre<sup>+</sup>-fur<sup>w<sup>t</sup>/Δfllox</sup>* mice, yielded various genotypes, including *P1<sup>+</sup>-Mcre<sup>+</sup>-fur<sup>fllox/Δfllox</sup>* (*PLAG1* transgenic and *fur* knockout in salivary glands and other MMTV-promoter-targeted cell lineages as discussed below), *P1<sup>+</sup>-Mcre<sup>+</sup>-fur<sup>w<sup>t</sup>/fllox</sup>* (*PLAG1* transgenic and *fur* heterozygote in salivary glands and other MMTV-promoter-targeted cell lineages), *P1<sup>+</sup>-Mcre<sup>+</sup>-fur<sup>w<sup>t</sup>/Δfllox</sup>* (*PLAG1* transgenic in salivary glands and other MMTV-promoter-targeted cell lineages and *fur* heterozygote in all cells) and *P1<sup>+</sup>-Mcre<sup>+</sup>-fur<sup>w<sup>t</sup>/wt</sup>* mice (*PLAG1* transgenic in salivary glands and other MMTV-promoter-targeted cell lineages and *fur* wild-type in all cells) as the most important ones relevant for the study presented here. In parallel, crosses with *fur<sup>w<sup>t</sup>/fllox</sup>* homozygous *PLAG1* transgenic mice and *fur<sup>w<sup>t</sup>/Δfllox</sup>* homozygous *MMTV-cre* transgenic mice were set up, to generate more offspring with the desired genotypes for further analysis of the impact of *fur* inactivation on *PLAG1*-induced tumor formation.

*Genotyping the mice by PCR analysis.* Genotyping the mice for *PLAG1* was conducted by PCR analysis on tail DNA using oligonucleotide primers *POS-1599* (5'-TTCTCAAGCATCGTCATCAT-3') and  $\beta$ -*globin* (5'-AAAATTCCAACACACTATTGC-3') at an annealing temperature of 58°C. PCR analysis was also used to genotype the mice for *cre* using the oligonucleotide primers *cre-1* (5'-CCTGTTTTGCACGTCACCG-3') and *cre-3* (5'-ATGCTTCTGTCCGTTTCCG-3') at an annealing temperature of 55°C. To genotype the mice for *fur*, tail DNA was PCR analyzed with *primer 1*

(5'-GCTGTATTTATTCCGGAGAC-3'), primer 2 (5'-GTA GTTAGGAGCACATACTG-3') and primer 4 (5'-AATCT GTTCCCTGCTGAGGA-3'). Primers 1 and 2 were used to discriminate between the *fur*<sup>wt</sup> allele (product of 219 bp) and the *fur*<sup>fllox</sup> allele (product of 311 bp), while primers 1 and 4 were used to identify the *fur*<sup>Δfllox</sup> allele (product of 322 bp) at an annealing temperature of 58°C, as described (15).

**RNA isolation from salivary glands and salivary gland tumors and cDNA preparation.** Total RNA from salivary glands and salivary gland tumors was isolated using the NucleoSpin RNA L Kit of Macherey-Nagel. Total RNA (2.5 μg) was reverse transcribed using random hexamer primers and M-MLV reverse transcriptase from Invitrogen in a volume of 20 μl.

**Quantitative real-time PCR (QRT-PCR) analysis.** QRT-PCR was performed with the MyIQ System (BioRad), in triplicate and using the comparative threshold cycle method. In all cases, 40 cycles of annealing/extension for 1 min at 60°C were performed. QRT-PCR products were detected using SYBR-Green. QRT-PCR for *glyceraldehyde 3-phosphate dehydrogenase (GAPDH)* was used as a reference to correct for sample quantity (forward primer, 5'-ATGGCCTTCCGTGTTCCCT-3' and reverse primer, 5'-CAGGCGGCACGTCAGAT-3'). For the study presented here, gene-specific primers were designed for *fur* (forward, 5'-CAGAAGCATGGCTTCCAC AAC-3' and reverse, 5'-TGTCCTGCTCTGTGCCAGAA-3') and *cre* (forward, 5'-CCGTACACAAAATTTGCCTG-3' and reverse, 5'-CCTCATCACTCGTTGCATCG-3').

**Histopathology.** For histopathology, salivary glands, salivary gland tumors and lymph nodes were removed carefully, fixed overnight in 4% formaldehyde and embedded in paraffin using routine procedures. Paraffin sections (5 μm) were stained with haematoxylin and eosin (H&E).

**B- and T-cell isolation, RNA isolation and cDNA preparation from lymph nodes.** CD4<sup>+</sup> cells were obtained from lymph nodes by positive selection using anti-CD4-coated magnetic beads (Dynal) according to the manufacturer's protocol. Beads were removed from the cells using Detachabead (Dynal) and a Dynal MPC-6 magnet (Dynal). Isolation of CD8<sup>+</sup> and CD19<sup>+</sup> cells was performed using the MACS CD8a<sup>+</sup> T-cell and B-cell Isolation Kits (Miltenyi Biotec), respectively. Lymph node cells were labeled with the appropriate negative selection biotin-antibody cocktail and then incubated with anti-biotin microbeads. Beads with unwanted labeled cells attached were removed using MS separation columns (Miltenyi Biotec). Cell purity was assessed by fluorescence-activated cell sorting (FACS). Cells were stained with PerCp-labeled anti-CD4, PE-labeled anti-CD8 and FITC-labeled anti-CD19 monoclonal antibodies (BD Pharmingen). The cells were analyzed on FACScalibur using CellQuest software (BD Biosciences). Total RNA from isolated CD4<sup>+</sup>, CD8<sup>+</sup> and CD19<sup>+</sup> cells was prepared using the RNeasy Mini Kit and DNase, as described by the manufacturer Qiagen. Total RNA (1 μg) was reverse transcribed using random hexamer primers and M-MLV reverse transcriptase from Invitrogen in a volume of 20 μl.

**Immunohistochemistry.** Immunostainings were conducted on 5-μm paraffin sections according to standard procedures. Briefly, after antigen retrieval in Tris/EDTA (10 mM, pH 9.0) for smooth muscle actin (SMA) or in citrate buffer (0.01 M, pH 6.0) for cytokeratin 8/18 (CK8/18), the mouse anti-human SMA antibody coupled to horseradish peroxidase (incubation 1 h, undiluted, EPOS clone1A4 from Dako) and the guinea pig anti-human CK8/18 antibody (incubation 30 min, 1:400, Progen) were used as primary antibodies. These are frequently used to stain myoepithelial and epithelial cells, respectively. For SMA, the antibody was visualized using 3,3'-diaminobenzidine (Dako real, code K5007). As a secondary reagent to detect CK8/18, a rabbit anti-guinea pig antibody (1:100, Dako) was used followed by the application of a tertiary swine anti-rabbit antibody coupled to horseradish peroxidase (1:100, Dako), and for visualization, 3,3'-diaminobenzidine was used.

## Results

*Fur is efficiently inactivated in the salivary glands of Mcre<sup>+</sup>-fur<sup>fllox/Δfllox</sup> mice and this causes smaller, but histologically normal salivary glands.* The aim of our study was to evaluate the impact of the absence of furin in the development of *PLAG1*-induced salivary gland tumorigenesis in genetically modified mice. In the control studies, we first evaluated the impact of the inactivation of *fur* without overexpression of *PLAG1* in *Mcre<sup>+</sup>-fur<sup>fllox/Δfllox</sup>* mice. In order to generate *Mcre<sup>+</sup>-fur<sup>fllox/Δfllox</sup>* mice, a crossing was established as described in Materials and methods.

Efficiency of removal of exon 2 of *fur* in the salivary glands of conditional *fur* knockout mice using the *MMTV-cre* system, was determined by QRT-PCR (Fig. 1A). The expression level of *fur* mRNA in the salivary glands of 10 week-old female *Mcre<sup>+</sup>-fur<sup>fllox/Δfllox</sup>* mice (*fur* knockout in salivary glands and other MMTV-promoter-targeted cell lineages as discussed below) was reduced to 4.2% as compared to the expression level in the salivary glands of female littermate *Mcre<sup>+</sup>-fur<sup>wt/fllox</sup>* mice (*fur* wild-type in all cells). In the salivary glands of female *Mcre<sup>+</sup>-fur<sup>wt/fllox</sup>* (*fur* heterozygote in salivary glands and other MMTV-promoter-targeted cell lineages) and *Mcre<sup>+</sup>-fur<sup>fllox/Δfllox</sup>* (*fur* heterozygote in all cells) littermates, *fur* mRNA levels were detected which were 63.8 and 55.4%, respectively, relative to *Mcre<sup>+</sup>-fur<sup>wt/fllox</sup>* mice.

Upon visual inspection of *Mcre<sup>+</sup>-fur<sup>fllox/Δfllox</sup>* mice, smaller salivary glands were observed (Fig. 1B and C). Therefore, the weight of the salivary glands of mice of all 4 genotypes was determined to investigate the impact of conditional inactivation of *fur* on the development of the salivary glands (Fig. 1D). The average weight of the salivary glands of female *Mcre<sup>+</sup>-fur<sup>fllox/Δfllox</sup>* mice of 6 to 10 weeks old was significantly lower than in sex-matched *Mcre<sup>+</sup>-fur<sup>wt/fllox</sup>* littermates (0.063 versus 0.093 g, n=8, p=0.022 using a two-sided Student's t-test with equal variance). In female (conditional) *fur* heterozygote *Mcre<sup>+</sup>-fur<sup>wt/fllox</sup>* and *Mcre<sup>+</sup>-fur<sup>fllox/Δfllox</sup>* littermates, no significant difference in average weight was found (0.090 and 0.088 g, respectively, n=8, p=0.873 and p=0.721, respectively, using a two-sided Student's t-test with equal variance).

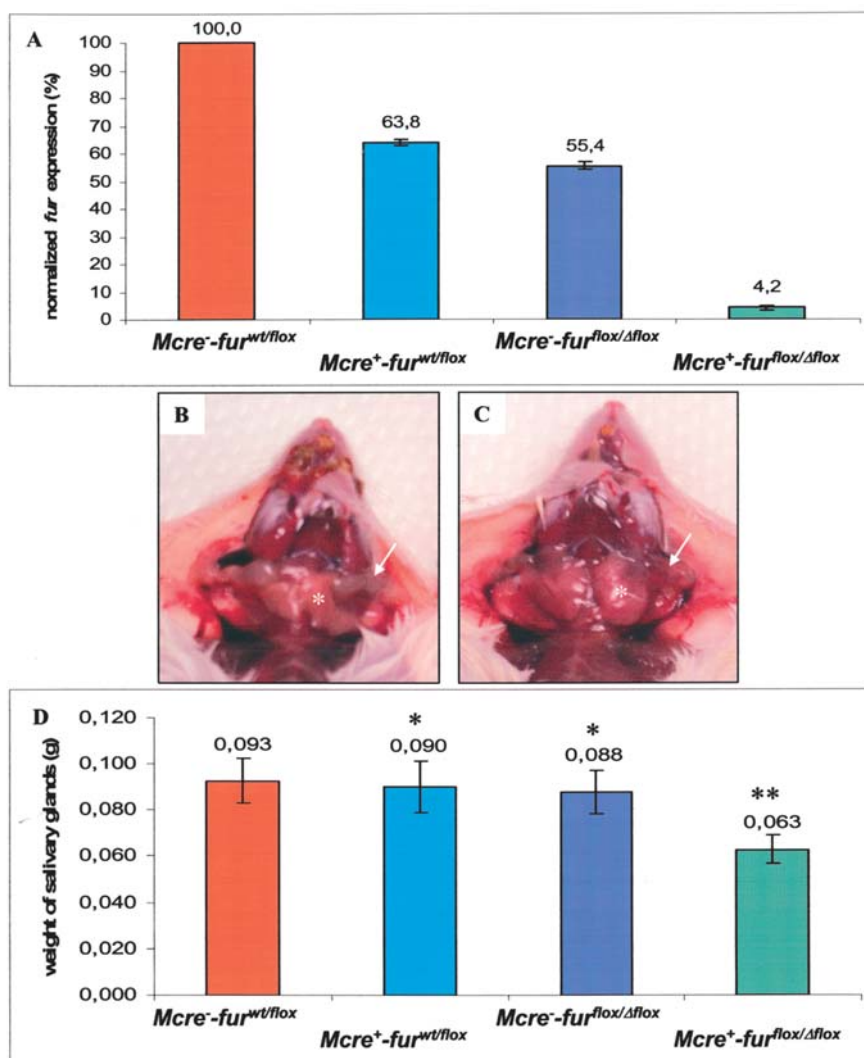


Figure 1. (A) QRT-PCR analysis of *fur* mRNA levels in salivary glands, comparing female *McCre-fur<sup>wt/flox</sup>* (red), *McCre<sup>+</sup>-fur<sup>wt/flox</sup>* (light blue), *McCre-fur<sup>flox/Δflox</sup>* (dark blue) and *McCre<sup>+</sup>-fur<sup>flox/Δflox</sup>* (green) mice of 10 weeks old. QRT-PCR experiments were performed in triplicate, using the comparative threshold cycle method and normalization relative to the mRNA levels of the housekeeping gene *GAPDH*. Average normalized values of 4 mice (littermates for each genotype) and the standard errors of the mean are indicated. (B) Picture of the ventral neck region after necropsy of a male *McCre<sup>+</sup>-fur<sup>flox/Δflox</sup>* mouse of 10 weeks old. The salivary glands (asterisk) were smaller and the cervical lymph nodes (arrow) were enlarged. Ten mice were evaluated and all displayed this profile. (C) Picture of the ventral neck region after necropsy of a male *McCre-fur<sup>wt/flox</sup>* mouse of 10 weeks old, littermate of the mouse in B. The salivary glands (asterisk) and cervical lymph nodes (arrow) had a normal size. Ten mice were evaluated and all had normal size salivary glands and cervical lymph nodes. (D) The average weight of the salivary glands of female *McCre-fur<sup>wt/flox</sup>*, *McCre<sup>+</sup>-fur<sup>wt/flox</sup>*, *McCre-fur<sup>flox/Δflox</sup>* and *McCre<sup>+</sup>-fur<sup>flox/Δflox</sup>* mice of 6-10 weeks old. The average weight of the salivary glands of 8 mice (littermates for each genotype) and the standard errors of the mean are indicated. \* $p > 0.05$  and \*\* $p < 0.05$ , using a two-sided Student's t-test with equal variance.

Histological analysis of several areas of the salivary glands of male and female *McCre<sup>+</sup>-fur<sup>flox/Δflox</sup>* and *McCre-fur<sup>wt/flox</sup>* mice revealed no apparent differences (Fig. 2A and B). The structure of mucous acini, serous acini, intercalated ducts, striated ducts and interlobular ducts in *McCre<sup>+</sup>-fur<sup>flox/Δflox</sup>* mice was similar to that of the sex-matched littermate control *McCre-fur<sup>wt/flox</sup>* mice ( $n=10$ ). The same histological results were obtained with the salivary glands of *McCre<sup>+</sup>-fur<sup>wt/flox</sup>* and *McCre-fur<sup>flox/Δflox</sup>* mice (data not shown), in which one *fur* allele was (conditionally) inactivated ( $n=10$ ).

*MMTV-cre-mediated fur inactivation causes enlarged cervical lymph nodes with activated follicles.* Most *McCre<sup>+</sup>-fur<sup>flox/Δflox</sup>* mice that did get born (males and females) died within 5-12 weeks after birth. They generally appeared in poor health.

They developed coarse hair presumably due to impaired grooming (Fig. 3A). The control *McCre-fur<sup>wt/flox</sup>* littermates were in good health (Fig. 3B). For *McCre<sup>+</sup>-fur<sup>flox/Δflox</sup>* mice, there was no significant difference in body weight, compared to the control sex-matched *McCre-fur<sup>wt/flox</sup>* littermates (data not shown) ( $n > 10$ ). *McCre<sup>+</sup>-fur<sup>wt/flox</sup>* and *McCre-fur<sup>flox/Δflox</sup>* mice appeared to be healthy (data not shown) ( $n > 10$ ).

At necropsy of *McCre<sup>+</sup>-fur<sup>flox/Δflox</sup>* mice, it was noticed that the lymph nodes close to the salivary glands were enlarged compared to the control *McCre-fur<sup>wt/flox</sup>* sex-matched littermates (Fig. 1B and C, respectively). Therefore, histological analysis of these cervical lymph nodes was performed. The lymph nodes of *McCre<sup>+</sup>-fur<sup>flox/Δflox</sup>* mice contained activated B follicles, which were not observed in *McCre-fur<sup>wt/flox</sup>* mice; Fig. 3C and D, respectively. Very large B follicles with a prominent

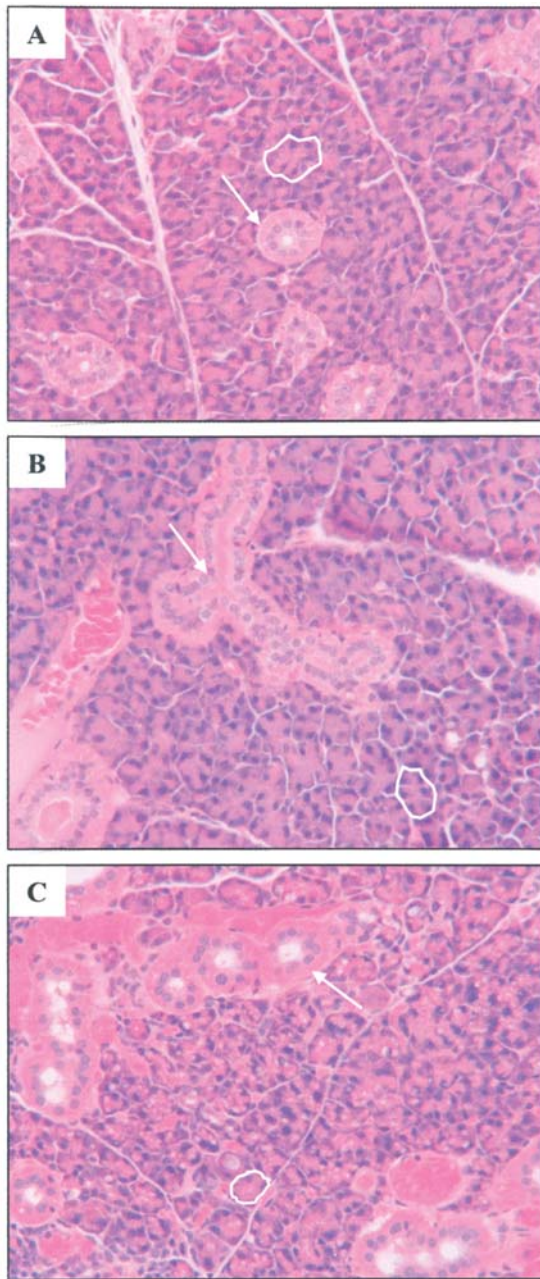


Figure 2. (A) Histology (H&E staining) of a salivary gland of a female  $Mcre^+fur^{fllox/Dfllox}$  mouse of 10 weeks old (original magnification x200). The histology, as far as could be assessed, seemed completely normal. The circle indicates a serous acinus and the arrow indicates a duct. Ten mice (males and females) were analyzed and all had a normal histology of the salivary glands. (B) Histology (H&E staining) of a salivary gland of a female  $Mcre^-fur^{wtfllox}$  mouse of 10 weeks old, littermate of the mouse in A (original magnification x200). The circle indicates a serous acinus and the arrow indicates a duct. Ten mice (males and females) were analyzed and all had a normal histology of the salivary glands. (C) Histology (H&E staining) of a salivary gland of the female  $PI^{+/-}Mcre^+fur^{fllox/Dfllox}$  mouse of 10 weeks old (original magnification x200). The histology, as far as could be assessed, seemed completely normal and none of the characteristic features of *PLAG1*-induced salivary gland pleomorphic adenoma was present. Neither were the characteristics of *PLAG1*-induced early tumoral stages present. The circle indicates a serous acinus and the arrow indicates a duct. B can be taken as a normal control.

germinal center and T-cell zones were present in respectively the cortex and paracortex of the cervical lymph nodes of  $Mcre^+fur^{fllox/Dfllox}$  mice. All  $Mcre^+fur^{fllox/Dfllox}$  mice analyzed,

displayed this activated profile of the cervical lymph node cells (n=10). The other lymph nodes in the body of  $Mcre^+fur^{fllox/Dfllox}$  mice were investigated and were also enlarged (data not shown) (n=10). The poor health condition and enlargement and activation of the lymph nodes point toward an impact of *fur* inactivation on the immunological system, probably causing a hyperactive immune system. The cervical and other lymph nodes of  $Mcre^+fur^{wtfllox}$  and  $Mcre^-fur^{fllox/Dfllox}$  mice had a normal size and normal histology (data not shown) (n=10).

The observed phenotype in the cervical lymph nodes of *MMTV-cre* transgenic conditional *fur* knockout mice is in accordance with the described *MMTV*-promoter-driven *cre* expression in B- and T-cells (28). To confirm that *fur* mRNA levels were affected in these cell populations of the lymph nodes of  $Mcre^+fur^{fllox/Dfllox}$  mice, *fur* expression was analyzed in the T-helper cells (Th), the T-cytotoxic cells (Tc) and the B-cells of the lymph nodes of a male  $Mcre^+fur^{fllox/Dfllox}$  mouse and a sex-matched littermate  $Mcre^-fur^{wtfllox}$  mouse. Therefore,  $CD4^+$ ,  $CD8^+$  and  $CD19^+$  cells were isolated, respectively. Cell purity was assessed by FACS analysis: 92-95% for  $CD4^+$  cells, 90-94% for  $CD8^+$  cells and ~70% for  $CD19^+$  cells. QRT-PCR analysis of *fur* expression was performed with normalization relative to *GAPDH* levels. In the Th-, Tc- and B-cells of an  $Mcre^+fur^{fllox/Dfllox}$  mouse, *fur* mRNA levels ranging from 11 to 23% of the levels in the Th-, Tc- and B-cells of a sex-matched littermate  $Mcre^-fur^{wtfllox}$  mouse were found (data not shown). *cre* expression was detected in all of these cell populations of an  $Mcre^+fur^{fllox/Dfllox}$  mouse, while no *cre* expression could be detected in an  $Mcre^-fur^{wtfllox}$  mouse (QRT-PCR data not shown).

**Underrepresentation of  $PI^{+/-}Mcre^+fur^{fllox/Dfllox}$  offspring.** To evaluate the role of furin in *PLAG1*-induced salivary gland tumorigenesis,  $PI^{+/-}Mcre^+fur^{fllox/Dfllox}$  mice were studied. In order to generate these compound mice with *MMTV-cre*-mediated *PLAG1* overexpression and *fur* inactivation,  $fur^{fllox/fllox}$  mice (15) were first crossed with PTMS1 (25), to generate  $PI^{+/-}fur^{wtfllox}$  mice, and in parallel *MMTV-cre* transgenic mice (28) were crossed with  $fur^{fllox/Dfllox}$  mice (15), to generate  $Mcre^{+/-}fur^{wtfllox}$  mice. Subsequently,  $PI^{+/-}fur^{wtfllox}$  mice were crossed with  $Mcre^{+/-}fur^{wtfllox}$  mice (Table I). According to Mendelian inheritance, 1/16 (6.3%) of the offspring should have been of the  $PI^{+/-}Mcre^+fur^{fllox/Dfllox}$  genotype. This subset appeared to be much smaller than expected however; only 1 mouse with this genotype was born from a total of 406 pups (0.2%); a female  $PI^{+/-}Mcre^+fur^{fllox/Dfllox}$  mouse.

Examination of the exact numbers of mice born per genotype, revealed that mice that were positive for *PLAG1* and *MMTV-cre* (red areas in Table I) were underrepresented ( $p=9.28165 \times 10^{-22}$ , Chi-square test).  $PI^{+/-}Mcre^+$  mice accounted for 4.3% (1.7+1.7+0.7+0.2%) while statistically, 25.0% was expected.  $Mcre^+fur^{fllox/Dfllox}$  mice were also underrepresented (underlined areas in Table I) in these crossings ( $p=7.76987 \times 10^{-6}$ , Chi-square test).

In parallel,  $PI^{+/-}fur^{wtfllox}$  mice were crossed with  $Mcre^{+/-}fur^{wtfllox}$  mice but this produced no  $PI^{+/-}Mcre^+fur^{fllox/Dfllox}$  offspring, out of 54. After crossing  $PI^{+/-}fur^{wtfllox}$  and  $Mcre^{+/-}fur^{wtfllox}$  mice, 1 male  $PI^{+/-}Mcre^+fur^{fllox/Dfllox}$  mouse was born, out of 22. Partial embryonic lethality in this background is

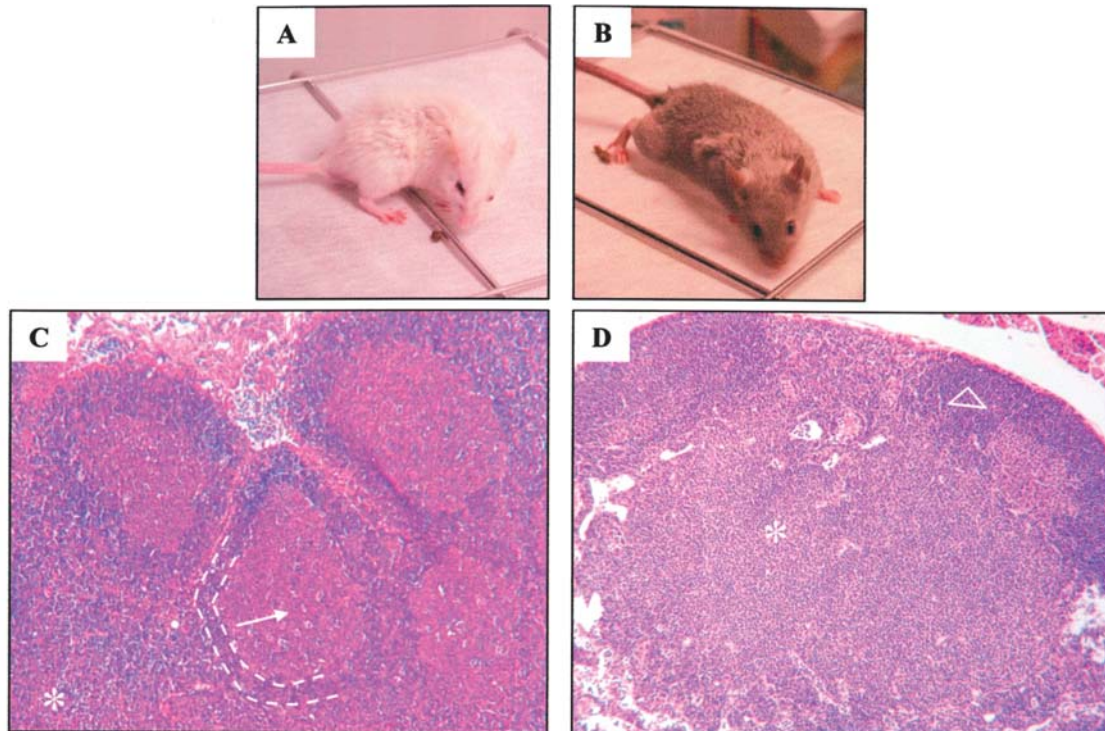


Figure 3. (A) Picture of a male *Mcre*<sup>+</sup>-*fur*<sup>flox/Δflox</sup> mouse of 10 weeks old. This mouse clearly was in poor health indicated by the coarse hair presumably due to impaired grooming. More than 10 mice were analyzed and all were in poor health. (B) Picture of a male *Mcre*<sup>-</sup>-*fur*<sup>wt/flox</sup> mouse of 10 weeks old, littermate of the mouse in A. This mouse was in normal health. More than 10 of these mice were analyzed and all were in normal health. (C) Histology (H&E staining) of a cervical lymph node of a male *Mcre*<sup>+</sup>-*fur*<sup>flox/Δflox</sup> mouse of 10 weeks old (original magnification x50). The histology showed very large B follicles with a prominent germinal center (arrow) and corona (area between the dotted lines), and T-cell zones (asterisk) present in the cortex and paracortex, respectively. All 10 histologically analyzed mice had activated cervical lymph node follicles. (D) Histology (H&E staining) of a cervical lymph node of a male *Mcre*<sup>-</sup>-*fur*<sup>wt/flox</sup> mouse of 10 weeks old, littermate of the mouse in C (original magnification x50). Histology showed a normal lymph node structure, with B follicles (triangle) which were not activated and T-cell zones (asterisk). This profile was confirmed in 9 other *Mcre*<sup>-</sup>-*fur*<sup>wt/flox</sup> mice.

Table I. Percentages of mice born from the crossing of *PI*<sup>+/-</sup>-*fur*<sup>wt/flox</sup> and *Mcre*<sup>+/-</sup>-*fur*<sup>wt/Δflox</sup> mice.<sup>a</sup>

n=406	<i>Mcre</i> <sup>+</sup>		<i>Mcre</i> <sup>-</sup>	
	<i>fur</i> <sup>wt</sup>	<i>fur</i> <sup>Δflox</sup>	<i>fur</i> <sup>wt</sup>	<i>fur</i> <sup>Δflox</sup>
<i>PI</i> <sup>+</sup>	1.7%	1.7%	9.4%	6.2%
<i>PI</i> <sup>-</sup>	0.7%	<u>0.2%</u> *	9.6%	10.6%
<i>PI</i> <sup>+</sup>	9.9%	6.2%	9.6%	8.9%
<i>PI</i> <sup>-</sup>	8.1%	<u>4.9%</u> *	6.9%	5.4%

<sup>a</sup>Vertically indicated are the possible genotypes resulting from a *PI*<sup>+/-</sup>-*fur*<sup>wt/flox</sup> parent, and horizontally indicated are the possible genotypes resulting from an *Mcre*<sup>+/-</sup>-*fur*<sup>wt/Δflox</sup> parent. Mice, 406 in total, were born and genotyped. The percentages of born mice per genotype are indicated. These percentages were very diverse, while statistically 6.3% (1/16) was expected for each genotype. *PI*<sup>+</sup>-*Mcre*<sup>+</sup> mice (red areas) were underrepresented, as well as *Mcre*<sup>+</sup>-*fur*<sup>flox/Δflox</sup> mice (underlined areas). The asterisk indicates that these mice were in poor health during their life.

the most likely explanation, as resorbed embryos were repeatedly observed in the uterus of the mothers. The number of normal *PI*<sup>+</sup>-*Mcre*<sup>+</sup> and *Mcre*<sup>+</sup>-*fur*<sup>flox/Δflox</sup> embryos together with the number of resorbed embryos was roughly in accordance with the number of expected *PI*<sup>+</sup>-*Mcre*<sup>+</sup> and *Mcre*<sup>+</sup>-*fur*<sup>flox/Δflox</sup> embryos (data not shown).

*PLAG1*-induced tumorigenesis in the salivary glands of *PI*<sup>+</sup>-*Mcre*<sup>+</sup>-*fur*<sup>flox/Δflox</sup> mice is considerably delayed. The female *PI*<sup>+</sup>-*Mcre*<sup>+</sup>-*fur*<sup>flox/Δflox</sup> mouse was sacrificed at 10 weeks after birth because of poor health. In this mouse, enlarged cervical lymph nodes with activated follicles were found, similar to those observed in *Mcre*<sup>+</sup>-*fur*<sup>flox/Δflox</sup> mice (data not shown). It did not have a macroscopically visible salivary gland tumor, while 100% of the *PI*<sup>+</sup>-*Mcre*<sup>+</sup>-*fur*<sup>wt/wt</sup> mice in this background had a macroscopically visible salivary gland tumor at 9 weeks, and >90% at 7 weeks (n=14) (see below). The histology of the salivary glands, as far as could be assessed, was normal (Fig. 2C), and none of the features characteristic of *PLAG1*-induced pleomorphic adenoma (25) was present. Neither were characteristics of *PLAG1*-induced early tumoral stages (25) observed.

The male *PI*<sup>+</sup>-*Mcre*<sup>+</sup>-*fur*<sup>flox/Δflox</sup> mouse was sacrificed at 40 weeks after birth. This mouse had been in poor health throughout its entire life. Enlarged cervical lymph nodes with activated follicles were present (data not shown). No tumor in the ventral neck region could macroscopically be detected. Histological analysis however showed characteristics similar

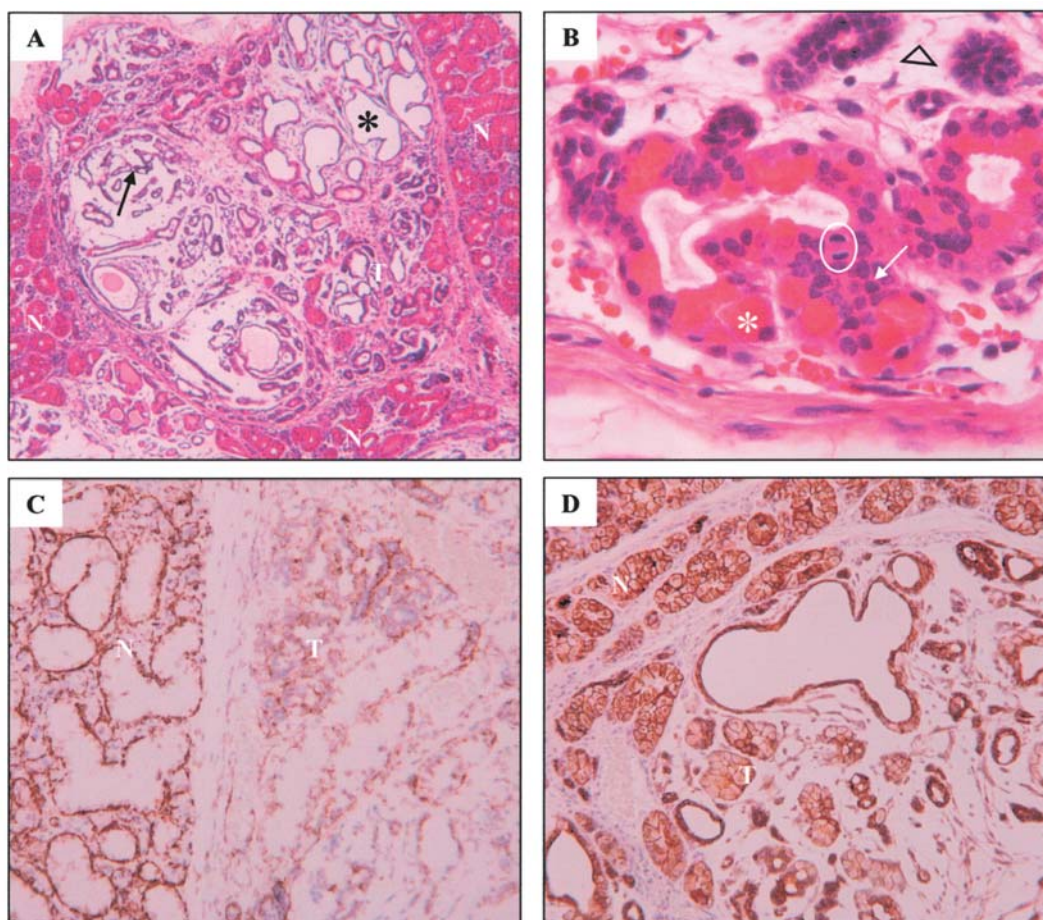


Figure 4. (A) Histology (H&E staining) of an early salivary gland tumor of a male  $PI^+Mcre^+fur^{flox/\Delta flox}$  mouse of 40 weeks old (original magnification x50). The early tumor resembled an early stage of *PLAG1*-induced salivary gland pleomorphic adenoma (25), with irregular, tubular structures (arrow) and dilated ducts (asterisk). Some normal parts (N) surrounded the early tumoral part (T). (B) Histology (H&E staining) of an early salivary gland tumor of a male  $PI^+Mcre^+fur^{flox/\Delta flox}$  mouse of 40 weeks old (original magnification x400). Some malformed acini-like structures were present (asterisk). A mitotic figure was present, indicated by the circle. Multilayered epithelium (arrow) and loose myxoid stroma (triangle) were also present. (C) Immunohistochemistry for SMA on an early salivary gland tumor of a male  $PI^+Mcre^+fur^{flox/\Delta flox}$  mouse of 40 weeks old (original magnification x100). The structure of a part of this salivary gland was clearly disturbed and had features of an early tumor (T). Some normal parts (N) were also present. SMA was in this case a marker for myoepithelial cells. (D) Immunohistochemistry for CK8/18 on an early salivary gland tumor of a male  $PI^+Mcre^+fur^{flox/\Delta flox}$  mouse of 40 weeks old (original magnification x100). The structure of a part of this salivary gland was clearly disturbed and had early tumoral features (T). Some normal parts (N) were also present. CK8/18 staining indicated epithelial cells and this staining together with the staining for SMA in C showed the pleomorphic adenoma character of this tumor.

to an early tumoral stage of the salivary glands of *fur* wild-type  $PI^+Mcre$  mice (25). These features included irregular, tubular structures, dilated ducts, some malformed acini-like structures, multilayered epithelium, loose myxoid stroma and mitotic figures (Fig. 4A and B). Additionally, SMA and CK8/18 stainings of the  $PI^+Mcre^+fur^{flox/\Delta flox}$  salivary glands confirmed one of the characteristics of pleomorphic adenoma: the presence of both myoepithelial and epithelial cells (as illustrated in Fig. 4C and D, respectively).

*Delayed onset of PLAG1-induced salivary gland tumor formation in  $PI^+Mcre^+fur^{wt/flox}$  and  $PI^+Mcre^+fur^{wt/\Delta flox}$  mice.* While only two  $PI^+Mcre^+fur^{flox/\Delta flox}$  mice were born, a larger number of  $PI^+Mcre^+fur^{wt/flox}$  and  $PI^+Mcre^+fur^{wt/\Delta flox}$  mice could be obtained (males and females). Evaluation of the age before a tumor mass could be macroscopically detected in the ventral neck region of  $PI^+Mcre^+fur^{wt/flox}$  (n=12) and  $PI^+Mcre^+fur^{wt/\Delta flox}$  (n=14) mice, revealed a significant difference (p=0.008 and p=0.001, respectively; two-sided Mann-Whitney U test) compared to  $PI^+Mcre^+fur^{wt/wt}$  (n=14)

mice (Fig. 5A). As a control,  $PI^+Mcre^+fur^{wt/wt}$  mice were evaluated (n=14). Fig. 5B and C show H&E staining of a salivary gland tumor of a  $PI^+Mcre^+fur^{wt/flox}$  mouse of 10 weeks old. This salivary gland tumor is similar to pleomorphic adenoma of the salivary glands of  $PI^+Mcre^+fur^{wt/wt}$  mice with the typical characteristics as discussed in the introduction, and this was the case in all  $PI^+Mcre^+fur^{wt/flox}$  and  $PI^+Mcre^+fur^{wt/\Delta flox}$  mice salivary gland tumors (males and females).

## Discussion

In this study, we examined *MMTV-cre*-mediated inactivation of *fur*, concomitant with overexpression of a *PLAG1* proto-oncogene, in the salivary glands and other organs of genetically modified mice. Our study clearly shows that mice lacking 1 functional allele of *fur* develop *PLAG1*-induced salivary gland tumors significantly later than mice with 2 functional *fur* alleles. An even more striking effect was observed in 2 *fur*-deficient mice.

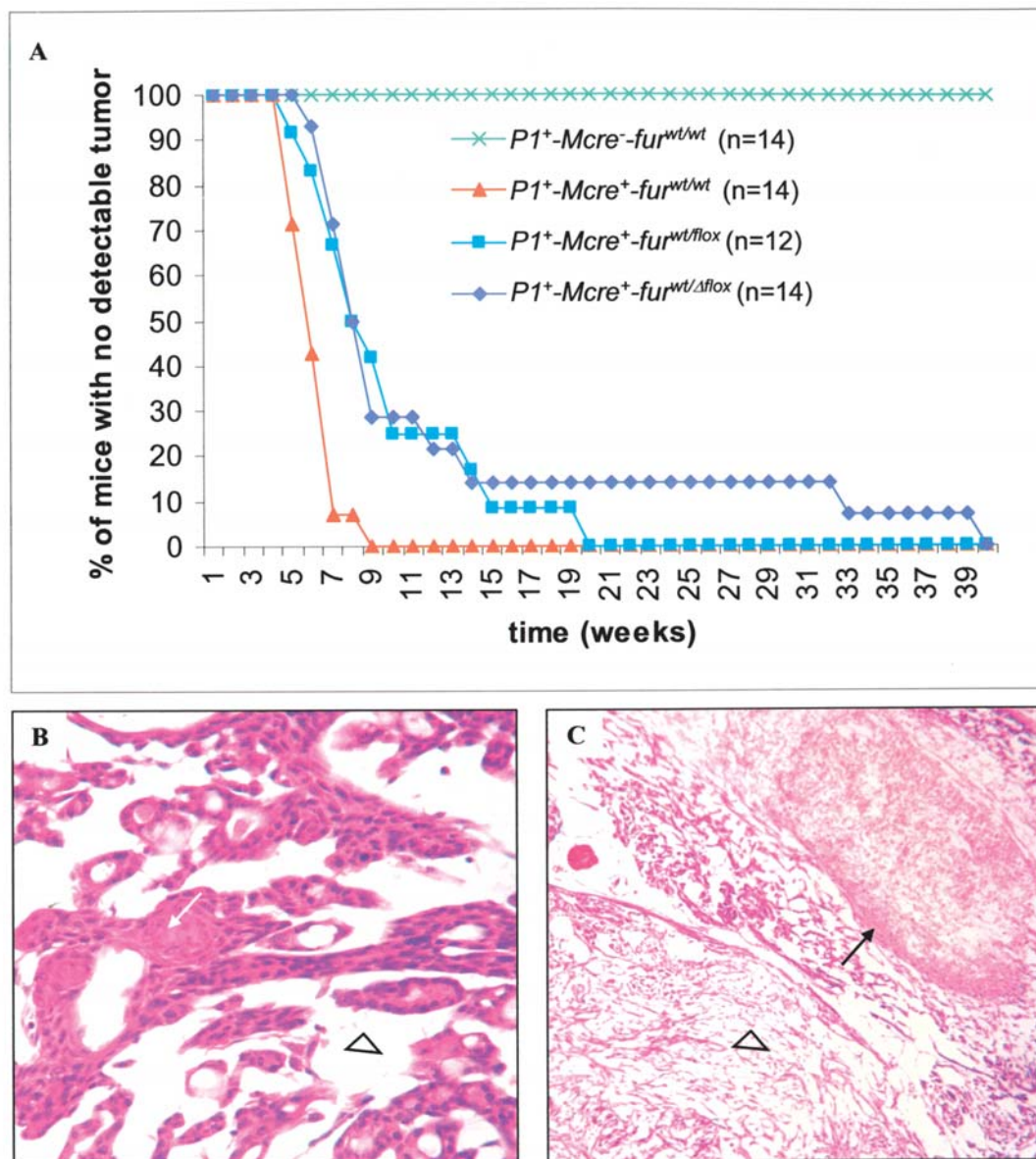


Figure 5. (A) Percentage of genetically modified mice with no macroscopically detectable tumor mass in the ventral neck region, as a function of their age. There was a significant ( $p=0.008$  and  $p=0.001$ , respectively) difference in macroscopically visible tumor onset between  $PI^+Mcre^+fur^{wt/wt}$  mice (red triangle curve) and  $PI^+Mcre^+fur^{wt/flox}$  mice (light blue square curve) or between  $PI^+Mcre^+fur^{wt/wt}$  mice and  $PI^+Mcre^+fur^{wt/\Delta flox}$  mice (dark blue diamond curve) (two-sided exact  $p$ -value from a Mann-Whitney U test). As a control,  $PI^+Mcre^-fur^{wt/wt}$  mice were evaluated (green cross curve). (B) Histology (H&E staining) of a salivary gland tumor of a female  $PI^+Mcre^+fur^{wt/flox}$  mouse of 10 weeks old (original magnification  $\times 200$ ). Characteristic features of *PLAG1*-induced salivary gland pleomorphic adenoma were present: multilayered epithelium with squamous differentiation and keratin pearls in the middle (arrow) and myxoid stroma (triangle). (C) Histology (H&E staining) of a salivary gland tumor of a female  $PI^+Mcre^+fur^{wt/flox}$  mouse of 10 weeks old (original magnification  $\times 50$ ). Myxoid stroma (triangle) is present in this pleomorphic adenoma and necrosis (arrow) is indicative of the malignant character of this tumor.

The salivary gland branching morphogenesis in mice starts at E11 and continues until puberty. Many key molecules in epithelial-mesenchymal cell interactions, branching morphogenesis and organogenesis are involved in the development of the salivary glands, such as EGF, FGF and TGF- $\beta$ . Furin has been suggested to be important in the proteolytic activation of these growth factors (29-32), which might explain the smaller size of the salivary glands in the conditional *fur* knockout mice. On the other hand, the architecture of the salivary glands was not affected by *fur* deficiency. This might suggest some functional redundancy probably provided by other PCs, as has been shown previously in the liver (15).

$Mcre^+fur^{flox/\Delta flox}$  mice had a nearly complete inactivation of the *fur* gene in the salivary glands. Only 4.2% of *fur* mRNA expression was observed as compared to  $Mcre^-fur^{wt/flox}$  mice. This residual level of *fur* expression might be due to the absence of *cre* expression in a small number of cells in the salivary glands. The slightly higher *fur* mRNA expression level in  $Mcre^+fur^{wt/flox}$  mice compared to  $Mcre^-fur^{flox/\Delta flox}$  mice, favors this explanation. In fact, in  $Mcre^-fur^{flox/\Delta flox}$  mice, monoallelic expression is germline transmitted and independent of *cre* expression.

$Mcre^+fur^{flox/\Delta flox}$  mice appeared to be in poor health and most of them died between 5-12 weeks after birth. The cervical lymph nodes of these mice were extremely large and

showed an activated profile; very large B follicles with a prominent germinal center were present. These mice probably had a hyperactive immune system.

Wagner *et al* described that when using the *MMTV-cre* system, *cre* is also expressed in the T- and B-cells (28), which would mean that *fur* is knocked out in these immune cells. QRT-PCR still showed fairly high *fur* mRNA levels in these immune cells of *Mcre<sup>+</sup>-fur<sup>flox/Dflox</sup>* mice (11-23%), and this may be due to the fact that isolation was not 100% pure or that *fur* was not knocked out in all of the Th-, Tc- and B-cells.

Recently, a possible role for furin in the immunological response was described by Pesu *et al* (33). They described that furin expression enhances interferon- $\gamma$  (IFN- $\gamma$ ) secretion, whereas inhibition of furin interfered with IFN- $\gamma$  production. Also, it was reported that TGF- $\beta$  plays an important role in the immune system (34-37) and since furin is the most important PC that can activate TGF- $\beta$  by endoproteolytic cleavage (29,32), it might be possible that in the *Mcre<sup>+</sup>-fur<sup>flox/Dflox</sup>* mice described here, TGF- $\beta$  processing was impaired and this could at least partially explain the immune phenotype of these mice.

Two *PI<sup>+</sup>-Mcre<sup>+</sup>-fur<sup>flox/Dflox</sup>* mice were born. The first *PI<sup>+</sup>-Mcre<sup>+</sup>-fur<sup>flox/Dflox</sup>* mouse was a female and was sacrificed at 10 weeks. At the histological level, no tumoral or early tumoral features were present in the salivary glands. The second *PI<sup>+</sup>-Mcre<sup>+</sup>-fur<sup>flox/Dflox</sup>* mouse was a male and the salivary gland morphology was evaluated at the age of 40 weeks. While macroscopically no tumor characteristics could be observed, early salivary gland tumor features were present. When we compared these 2 *PI<sup>+</sup>-Mcre<sup>+</sup>-fur<sup>flox/Dflox</sup>* mice with *PI<sup>+</sup>-Mcre<sup>+</sup>-fur<sup>wt/wt</sup>* mice that developed a macroscopically detectable salivary gland tumor after 6.4 weeks on average (Fig. 5A), there was a considerable delay in tumor onset in these 2 *PI<sup>+</sup>-Mcre<sup>+</sup>-fur<sup>flox/Dflox</sup>* mice. This suggests that furin plays an important role in *PLAG1*-induced salivary gland tumorigenesis.

The fact that only 2 *PI<sup>+</sup>-Mcre<sup>+</sup>-fur<sup>flox/Dflox</sup>* mice were born, was most likely due to partial embryonic lethality of *PI<sup>+</sup>-Mcre<sup>+</sup>* and *Mcre<sup>+</sup>-fur<sup>flox/Dflox</sup>* mice in this background, as resorbed embryos were found in the uterus of the mothers, as discussed above. Since this underrepresentation of *PI<sup>+</sup>-Mcre<sup>+</sup>* mice was not observed in the direct crossing of PTMS1 and *MMTV-cre* mice, as previously described (25), this underrepresentation was most likely due to the mixed background caused by crossing with the *fur*-modified mice. These *fur*-modified mice have a mixed background. A similar partial embryonic lethality of *PI<sup>+</sup>-Mcre<sup>+</sup>* mice was observed when crosses were made with *igf2<sup>p-im</sup>* mice, which also have a mixed background (Declercq *et al*, unpublished results). Since general *PLAG1* overexpression and also general *fur* knockout is embryonically lethal (14,25), it is possible that in the background of the crosses described in this study, *cre* expression was in some mice more widespread or started at an earlier stage. Therefore, it is possible that in some of these mice, *PLAG1* was overexpressed and *fur* was knocked out in a more general pattern than in other mice. The *MMTV-promoter* system was described to drive expression in a very broad pattern (28). Backcrossing to a homogeneous background is currently being performed, which might overcome the partial embryonic lethality.

A significant delay in tumor onset was also observed in *PI<sup>+</sup>-Mcre<sup>+</sup>-fur<sup>wt/flox</sup>* and *PI<sup>+</sup>-Mcre<sup>+</sup>-fur<sup>wt/Dflox</sup>* mice as compared to *PI<sup>+</sup>-Mcre<sup>+</sup>-fur<sup>wt/wt</sup>* mice. This indicates that haplo-insufficiency of *fur* was sufficient to have an impact on *PLAG1*-induced salivary gland tumorigenesis. Hemizyosity of several other enzymes, such as *PCI* was also reported to result in a phenotype (38). The morphology of the salivary gland tumors that *PI<sup>+</sup>-Mcre<sup>+</sup>-fur<sup>wt/flox</sup>* and *PI<sup>+</sup>-Mcre<sup>+</sup>-fur<sup>wt/Dflox</sup>* mice eventually developed, was similar to the morphology of *PLAG1*-induced pleomorphic adenoma of the salivary glands in *PI<sup>+</sup>-Mcre<sup>+</sup>-fur<sup>wt/wt</sup>* mice.

At present, the molecular pathways involved in *PLAG1*-induced salivary gland tumorigenesis, are not fully elucidated. Nevertheless, there are some indications that IGF-2/IGF-1R signaling might play a role in *PLAG1*-induced salivary gland tumorigenesis. Indeed, *insulin-like growth factor 2 (igf2)*, one of the direct target genes of *PLAG1*, is highly upregulated in *PLAG1*-induced salivary gland tumors (25,39). Furthermore, *IGF-1R*-negative cells cannot be transformed via transduction of DNA expressing high levels of *PLAG1* (40). Notably, IGF-2 and IGF-1R can both be cleaved by furin, at least *in vitro* (9,41,42). Nevertheless it cannot be excluded that other furin substrates such as growth factors like TGF- $\beta$ , PDGF, or adhesion molecules like integrins or angiogenic factors like VEGF or (membrane-type) matrix metalloproteinases, which play an important role in tumorigenesis (5,7,29,32,43-45), are involved. Further analysis of *PI<sup>+</sup>-Mcre<sup>+</sup>-fur<sup>flox/Dflox</sup>* mice is necessary to further elucidate the molecular mechanisms that lead to the delay in tumor formation.

In conclusion, this study demonstrates that inactivation of *fur* considerably delays *PLAG1*-induced tumor development. Even heterozygous inactivation of *fur* is sufficient to significantly delay tumor onset, establishing the importance of furin in this process. However, the tumor still develops, suggesting a functional redundancy probably provided by other PCs. This study implies that furin could be a valuable therapeutic target to affect *PLAG1*-induced tumor development.

## Acknowledgements

We thank Christel Van den Broeck and Rob Deckers for the technical assistance. We also thank Steffen Fieuids (Biostatistical Center, University Hospital Leuven, Belgium) for the statistical advice. This research was supported by 'Geconcerteerde Onderzoeksactie' (GOA-08/016), the 'Fonds voor Wetenschappelijk Onderzoek Vlaanderen' grant (FWO-G.0099.02), the Cancer Research Program of Fortis Bank Insurance, the Foundation for Biochemical and Pharmaceutical Research and Education, and the Belgian Federation against Cancer.

## References

1. Bassi DE, Fu J, Lopez de Cicco R and Klein-Szanto AJ: Proprotein convertases: 'master switches' in the regulation of tumor growth and progression. *Mol Carcinog* 44: 151-161, 2005.
2. Bassi DE, Mahloogi H and Klein-Szanto AJ: The proprotein convertases furin and PACE4 play a significant role in tumor progression. *Mol Carcinog* 28: 63-69, 2000.
3. Khatib AM: Regulation of carcinogenesis, angiogenesis and metastasis by the proprotein convertases (PCs): a new potential strategy in cancer therapy. Springer, Dordrecht, 2006.

4. Khatib AM, Bassi D, Siegfried G, Klein-Szanto AJ and Ouafik L: Endo/exo-proteolysis in neoplastic progression and metastasis. *J Mol Med* 83: 856-864, 2005.
5. Khatib AM, Siegfried G, Chretien M, Metrakos P and Seidah NG: Proprotein convertases in tumor progression and malignancy: novel targets in cancer therapy. *Am J Pathol* 160: 1921-1935, 2002.
6. Lopez de Cicco R, Watson JC, Bassi DE, Litwin S and Klein-Szanto AJ: Simultaneous expression of furin and vascular endothelial growth factor in human oral tongue squamous cell carcinoma progression. *Clin Cancer Res* 10: 4480-4488, 2004.
7. Bassi DE, Lopez De Cicco R, Mahloogi H, Zucker S, Thomas G and Klein-Szanto AJ: Furin inhibition results in absent or decreased invasiveness and tumorigenicity of human cancer cells. *Proc Natl Acad Sci USA* 98: 10326-10331, 2001.
8. Lopez de Cicco R, Bassi DE, Benavides F, Conti CJ and Klein-Szanto AJ: Inhibition of proprotein convertases: approaches to block squamous carcinoma development and progression. *Mol Carcinog* 46: 654-659, 2007.
9. Khatib AM, Siegfried G, Prat A, Luis J, Chretien M, Metrakos P and Seidah NG: Inhibition of proprotein convertases is associated with loss of growth and tumorigenicity of HT-29 human colon carcinoma cells: importance of insulin-like growth factor-1 (IGF-1) receptor processing in IGF-1-mediated functions. *J Biol Chem* 276: 30686-30693, 2001.
10. Liu B, Amizuka N, Goltzman D and Rabbani SA: Inhibition of processing of parathyroid hormone-related peptide by anti-sense furin: effect *in vitro* and *in vivo* on rat Leydig (H-500) tumor cells. *Int J Cancer* 63: 276-281, 1995.
11. Lopez de Cicco R, Bassi DE, Zucker S, Seidah NG and Klein-Szanto AJ: Human carcinoma cell growth and invasiveness is impaired by the propeptide of the ubiquitous proprotein convertase furin. *Cancer Res* 65: 4162-4171, 2005.
12. Mercapide J, Lopez De Cicco R, Bassi DE, Castresana JS, Thomas G and Klein-Szanto AJ: Inhibition of furin-mediated processing results in suppression of astrocytoma cell growth and invasiveness. *Clin Cancer Res* 8: 1740-1746, 2002.
13. Bassi DE, Mahloogi H, Lopez De Cicco R and Klein-Szanto A: Increased furin activity enhances the malignant phenotype of human head and neck cancer cells. *Am J Pathol* 162: 439-447, 2003.
14. Roebroek AJ, Umans L, Pauli IG, Robertson EJ, van Leuven F, Van de Ven WJ and Constam DB: Failure of ventral closure and axial rotation in embryos lacking the proprotein convertase furin. *Development* 125: 4863-4876, 1998.
15. Roebroek AJ, Taylor NA, Louagie E, Pauli I, Smeijers L, Snellinx A, Lauwers A, Van de Ven WJ, Hartmann D and Creemers JW: Limited redundancy of the proprotein convertase furin in mouse liver. *J Biol Chem* 279: 53442-53450, 2004.
16. Van Dyck F, Declercq J, Braem CV and Van de Ven WJ: *PLAG1*, the prototype of the *PLAG* gene family: Versatility in tumour development (Review). *Int J Oncol* 30: 765-774, 2007.
17. Astrom AK, Voz ML, Kas K, Roijer E, Wedell B, Mandahl N, Van de Ven W, Mark J and Stenman G: Conserved mechanism of *PLAG1* activation in salivary gland tumors with and without chromosome 8q12 abnormalities: identification of SII as a new fusion partner gene. *Cancer Res* 59: 918-923, 1999.
18. Kas K, Voz ML, Roijer E, Astrom AK, Meyen E, Stenman G and Van de Ven WJ: Promoter swapping between the genes for a novel zinc finger protein and beta-catenin in pleiomorphic adenomas with t(3;8)(p21;q12) translocations. *Nat Genet* 15: 170-174, 1997.
19. Voz ML, Astrom AK, Kas K, Mark J, Stenman G and Van de Ven WJ: The recurrent translocation t(5;8)(p13;q12) in pleiomorphic adenomas results in upregulation of *PLAG1* gene expression under control of the *LIFR* promoter. *Oncogene* 16: 1409-1416, 1998.
20. Astrom A, D'Amore ES, Sainati L, Panarello C, Morerio C, Mark J and Stenman G: Evidence of involvement of the *PLAG1* gene in lipoblastomas. *Int J Oncol* 16: 1107-1110, 2000.
21. Hibbard MK, Kozakewich HP, Dal Cin P, Sciort R, Tan X, Xiao S and Fletcher JA: *PLAG1* fusion oncogenes in lipoblastoma. *Cancer Res* 60: 4869-4872, 2000.
22. Morerio C, Rapella A, Rosanda C, Tassano E, Gambini C, Romagnoli G and Panarello C: *PLAG1*-*HAS2* fusion in lipoblastoma with masked 8q intrachromosomal rearrangement. *Cancer Genet Cytogenet* 156: 183-184, 2005.
23. Zatkova A, Rouillard JM, Hartmann W, Lamb BJ, Kuick R, Eckart M, von Schweinitz D, Koch A, Fonatsch C, Pietsch T, Hanash SM and Wimmer K: Amplification and overexpression of the IGF2 regulator *PLAG1* in hepatoblastoma. *Genes Chromosomes Cancer* 39: 126-137, 2004.
24. Castilla LH, Perrat P, Martinez NJ, Landrette SF, Keys R, Oikemus S, Flanagan J, Heilman S, Garrett L, Dutra A, Anderson S, Pihan GA, Wolff L and Liu PP: Identification of genes that synergize with Cbfb-MYH11 in the pathogenesis of acute myeloid leukemia. *Proc Natl Acad Sci USA* 101: 4924-4929, 2004.
25. Declercq J, Van Dyck F, Braem CV, Van Valckenborgh IC, Voz M, Wassef M, Schoonjans L, Van Damme B, Fiette L and Van de Ven WJ: Salivary gland tumors in transgenic mice with targeted *PLAG1* proto-oncogene overexpression. *Cancer Res* 65: 4544-4553, 2005.
26. Zhao X, Ren W, Yang W, Wang Y, Kong H, Wang L, Yan L, Xu G, Fei J, Fu J, Zhang C and Wang Z: Wnt pathway is involved in pleiomorphic adenomas induced by overexpression of *PLAG1* in transgenic mice. *Int J Cancer* 118: 643-648, 2006.
27. Van Dyck F, Scroyen I, Declercq J, Sciort R, Kahn B, Lijnen R and Van de Ven WJ: AP2-Cre-mediated expression activation of an oncogenic *PLAG1* transgene results in cavernous angiomas in mice. *Int J Oncol* 32: 33-40, 2008.
28. Wagner KU, McAllister K, Ward T, Davis B, Wiseman R and Hennighausen L: Spatial and temporal expression of the Cre gene under the control of the MMTV-LTR in different lines of transgenic mice. *Transgenic Res* 10: 545-553, 2001.
29. Dubois CM, Blanchette F, Laprise MH, Leduc R, Grondin F and Seidah NG: Evidence that furin is an authentic transforming growth factor-beta1-converting enzyme. *Am J Pathol* 158: 305-316, 2001.
30. Fukumoto S: Post-translational modification of fibroblast growth factor 23. *Ther Apher Dial* 9: 319-322, 2005.
31. Jorgensen PE, Nexø E, Poulsen SS, Almendingen M and Berg T: Processing of epidermal growth factor in the rat submandibular gland by kallikrein-like enzymes. *Growth Factors* 11: 113-123, 1994.
32. Leitelin J, Aulwurm S, Waltereit R, Naumann U, Wagenknecht B, Garten W, Weller M and Platten M: Processing of immunosuppressive pro-TGF-beta 1,2 by human glioblastoma cells involves cytoplasmic and secreted furin-like proteases. *J Immunol* 166: 7238-7243, 2001.
33. Pesu M, Muul L, Kanno Y and O'Shea JJ: Proprotein convertase furin is preferentially expressed in T helper 1 cells and regulates interferon gamma. *Blood* 108: 983-985, 2006.
34. Kulkarni AB, Huh CG, Becker D, Geiser A, Lyght M, Flanders KC, Roberts AB, Sporn MB, Ward JM and Karlsson S: Transforming growth factor beta 1 null mutation in mice causes excessive inflammatory response and early death. *Proc Natl Acad Sci USA* 90: 770-774, 1993.
35. Li MO, Wan YY and Flavell RA: T cell-produced transforming growth factor-beta1 controls T cell tolerance and regulates Th1- and Th17-cell differentiation. *Immunity* 26: 579-591, 2007.
36. Li MO, Wan YY, Sanjabi S, Robertson AK and Flavell RA: Transforming growth factor-beta regulation of immune responses. *Annu Rev Immunol* 24: 99-146, 2006.
37. Nandula SR, Amarnath S, Molinolo A, Bandyopadhyay BC, Hall B, Goldsmith CM, Zheng C, Larsson J, Sreenath T, Chen W, Ambudkar IS, Karlsson S, Baum BJ and Kulkarni AB: Female mice are more susceptible to developing inflammatory disorders due to impaired transforming growth factor beta signaling in salivary glands. *Arthritis Rheum* 56: 1798-1805, 2007.
38. Zhu X, Zhou A, Dey A, Norrbom C, Carroll R, Zhang C, Laurent V, Lindberg I, Ugleholdt R, Holst JJ and Steiner DF: Disruption of *PC1/3* expression in mice causes dwarfism and multiple neuroendocrine peptide processing defects. *Proc Natl Acad Sci USA* 99: 10293-10298, 2002.
39. Voz ML, Mathys J, Hensen K, Pendeville H, Van Valckenborgh I, Van Huffel C, Chavez M, Van Damme B, De Moor B, Moreau Y and Van de Ven WJ: Microarray screening for target genes of the proto-oncogene *PLAG1*. *Oncogene* 23: 179-191, 2004.
40. Hensen K, van Valckenborgh IC, Kas K, van de Ven WJ and Voz ML: The tumorigenic diversity of the three *PLAG* family members is associated with different DNA binding capacities. *Cancer Res* 62: 1510-1517, 2002.

41. Duguay SJ, Jin Y, Stein J, Duguay AN, Gardner P and Steiner DF: Post-translational processing of the insulin-like growth factor-2 precursor. Analysis of O-glycosylation and endoproteolysis. *J Biol Chem* 273: 18443-18451, 1998.
42. Lehmann M, Andre F, Bellan C, Remacle-Bonnet M, Garrouste F, Parat F, Lissitsky JC, Marvaldi J and Pommier G: Deficient processing and activity of type I insulin-like growth factor receptor in the furin-deficient LoVo-C5 cells. *Endocrinology* 139: 3763-3771, 1998.
43. Lissitzky JC, Luis J, Munzer JS, Benjannet S, Parat F, Chretien M, Marvaldi J and Seidah NG: Endoproteolytic processing of integrin pro-alpha subunits involves the redundant function of furin and proprotein convertase (PC) 5A, but not paired basic amino acid converting enzyme (PACE) 4, PC5B or PC7. *Biochem J* 346: 133-138, 2000.
44. Siegfried G, Basak A, Cromlish JA, Benjannet S, Marcinkiewicz J, Chretien M, Seidah NG and Khatib AM: The secretory proprotein convertases furin, PC5, and PC7 activate VEGF-C to induce tumorigenesis. *J Clin Invest* 111: 1723-1732, 2003.
45. Siegfried G, Khatib AM, Benjannet S, Chretien M and Seidah NG: The proteolytic processing of pro-platelet-derived growth factor-A at RRKR(86) by members of the proprotein convertase family is functionally correlated to platelet-derived growth factor-A-induced functions and tumorigenicity. *Cancer Res* 63: 1458-1463, 2003.